

# Evidence for anisotropic triplet superconductor order parameter in half-metallic ferromagnetic $\text{La}_{0.7}\text{Ca}_{0.3}\text{Mn}_3\text{O}$ proximity coupled to superconducting $\text{Pr}_{1.85}\text{Ce}_{0.15}\text{CuO}_4$

Y. Kalcheim and O. Millo\*

*Racah Institute of Physics and the Hebrew University Center for Nanoscience and Nanotechnology, The Hebrew University of Jerusalem, Jerusalem 91904, Israel*

M. Egilmez, J. W. A. Robinson, and M. G. Blamire

*Department of Material Science and Metallurgy, University of Cambridge, Pembroke Street, Cambridge, CB2 3QZ, United Kingdom*

(Received 22 November 2011; published 7 March 2012)

Scanning tunneling spectroscopy measurements performed on  $\text{La}_{0.7}\text{Ca}_{0.3}\text{Mn}_3\text{O}$  (LCMO) films epitaxially grown on  $\text{Pr}_{1.85}\text{Ce}_{0.15}\text{CuO}_4$  (PCCO) reveal localized penetration of superconductivity into the LCMO up to distances much larger than is possible for Cooper pairs in a singlet spin state to exist. This long-range proximity effect is manifested in the tunneling spectra as gaps and, less abundantly, as zero-bias conductance peaks (ZBCPs). Since ZBCPs were not found on the bare PCCO films, their appearance is attributed to an anisotropic ( $p$  wave or  $d$  wave) triplet-pairing superconductor order parameter induced in the LCMO.

DOI: [10.1103/PhysRevB.85.104504](https://doi.org/10.1103/PhysRevB.85.104504)

PACS number(s): 74.45.+c, 74.55.+v, 74.20.Rp

## I. INTRODUCTION

Half metallic ferromagnetic (HMF) materials have been investigated in great detail over the past two decades, partly due to their possible application as sources of highly spin-polarized currents.<sup>1</sup> More recently, theoretical<sup>2,3</sup> and experimental<sup>4,5</sup> work has focused on the proximity coupling of HMF materials with superconductors to investigate the interplay between ferromagnetism and superconductivity.

At a normal metal-superconductor (S-N) junction with high interfacial transparency, the mechanism underlying the proximity effect is Andreev reflection (AR), where a holelike quasiparticle traveling in N is retroreflected from the N-S interface as an electronlike quasiparticle with opposite spin. These two quasiparticles become correlated in phase through the annihilation of a Cooper pair in the superconductor and diffusively propagate in N. Their phase coherence thus decays within a characteristic coherence length of  $\xi_N = \sqrt{\hbar D/k_B T}$  that can be as large as  $\sim 100$  nm at low temperatures (where  $D$  is the diffusivity of the normal metal and  $T$  is the temperature). For S-F junctions, the proximity effect is much shorter ranged due to the ferromagnetic exchange field acting differentially on the spins of the two quasiparticles.<sup>6,7</sup> This can be understood by analogy to the Fulde-Ferrel<sup>8</sup> and Larkin-Ovchinnikov<sup>9</sup> (FFLO) state in ferromagnetic superconductors. As the holelike and electronlike quasiparticles have opposite spins, they experience a difference in potential energy due to the exchange field ( $E_{\text{ex}}$ ) in F. This leads to the pairs having a nonzero center of mass momentum so that the wave function of a pair acquires an oscillating component superimposed on a rapid decay given by the ferromagnetic coherence length  $\xi_F = \sqrt{\hbar D/2E_{\text{ex}}}$  in the diffusive limit. For strong transition metal ferromagnets Ni,<sup>10,11</sup> Fe,<sup>12</sup> and Co,<sup>13</sup>  $\xi_F$  has been estimated to be  $\sim 1$  nm, while for weakly ferromagnetic alloys, such as CuNi<sup>14</sup> or PdNi,<sup>15,16</sup>  $\xi_F$  is obviously much larger,  $\sim 20$  and  $\sim 8$  nm, respectively. The material studied here, LCMO, has a quite large exchange energy of  $\sim 3$  eV and a rather small Fermi velocity of  $\sim 7 \times 10^7$  cm/s, and thus  $\xi_F$  is estimated to be no more than 1 nm.<sup>17</sup>

Proximity effects conforming to the above FFLO-type mechanism, with a superconducting penetration depth on the order of  $\xi_F$ , were experimentally observed in various S-F multilayer systems.<sup>18,19</sup> However, long-ranged S-F proximity effects have also been observed in a variety of ferromagnetic materials, including Ni wires<sup>20</sup> and Ni multilayers,<sup>21</sup> half metallic  $\text{CrO}_2$ ,<sup>4,22</sup> rare earth Ho,<sup>23</sup> Co wires,<sup>24</sup> Co multilayers,<sup>25</sup> and Ho/Co/Ho<sup>26</sup> layers; and intermetallic  $\text{Cu}_2\text{MnAl}$ .<sup>27</sup> A long-ranged proximity effect is possible according to theory if some form of inhomogeneous magnetism is present at the S-F interface so that Cooper pairs with parallel rather than antiparallel spins can form via a spin-mixing effect.<sup>28</sup> Spin-aligned Cooper pairs are in a triplet spin state, making them insensitive to the ferromagnetic exchange field, and can thus support a long-ranged proximity effect.

In the triplet spin state, the orbital symmetry of the induced order parameter (OP) in the ferromagnet can be either even ( $s$  or  $d$  wave) or odd ( $p$  or  $f$  wave), corresponding, respectively, to an odd or an even dependence on the Matsubara frequency.<sup>28</sup> Sign-changing anisotropic OPs such as  $p$  wave or  $d$  wave are known to result in states of zero energy at reflective interfaces or near impurities due to multiple (Andreev and normal) scattering events. Such so-called Andreev bound states accumulate at the Fermi energy and are detectable by scanning tunneling spectroscopy (STS) as zero-bias conductance peaks (ZBCPs) in the differential conduction ( $dI/dV$ ) vs voltage ( $V$ ) characteristics. Zero-bias conductance peaks are thus a hallmark of anisotropic pairing correlations and unconventional superconductivity. It is important to note that the anisotropic OPs are sensitive to impurity scattering<sup>29</sup> and are thus predicted to be less abundant than the more robust  $s$ -wave pairing component.

On the other hand, long-range proximity effect can also occur in F-S junctions by induction of superconducting correlations near domain walls in a process known as crossed Andreev reflections (CAREs).<sup>30,31</sup> Here, a holelike quasiparticle traveling in one magnetic domain is retroreflected as an electronlike quasiparticle of opposite spin in an adjacent

domain, thus overcoming the impeding effect of the exchange field. This mechanism, however, applies only when the domain wall width is comparable to the superconducting coherence length in  $S$ . Evidence for this was observed in  $\text{SrRuO}_3/\text{YBCO}$  bilayers.<sup>32</sup>

Recently, we performed STS on half metallic ferromagnetic LCMO grown on the hole-doped high-temperature superconductor  $\text{YBa}_2\text{Cu}_3\text{O}_{7-\delta}$  (YBCO). In this experiment, superconducting features, both gaps and ZBCPs, were observed in the  $dI/dV$ - $V$  tunneling spectra acquired on LCMO films up to thicknesses of 30 nm, therefore implying a long-ranged triplet proximity effect.<sup>5</sup> Crossed Andreev reflection was ruled out as a dominant effect in these junctions because the coherence length in YBCO ( $\sim 2$  nm) is much smaller than the known domain wall width in LCMO at low temperatures,  $\sim 20$  nm.<sup>33</sup> The fact that ZBCPs appeared in tunneling spectra pointed to an anisotropic ( $d$  or  $p$  wave) superconducting OP, possibly induced in the LCMO. However, because the ZBCPs were also observed in bare films of YBCO (a  $d$ -wave superconductor), it is not clear whether the ZBCPs on the LCMO surface reflect the effect of the anisotropic OP in the underlying YBCO film or manifest a genuine anisotropy of the induced triplet-pairing OP in the LCMO. The aim of this paper is to address this problem by replacing the YBCO with  $\text{Pr}_{1.85}\text{Ce}_{0.15}\text{CuO}_4$  (PCCO), an electron-doped high-temperature superconductor well known for being strongly in the dirty limit so ZBCPs are not detectable.<sup>34</sup> Consequently, observation of a long-ranged proximity effect yielding ZBCPs in the tunneling spectra of LCMO/PCCO bilayers would strongly support the picture that the triplet-pairing OP induced in the LCMO is intrinsically anisotropic.

## II. EXPERIMENTAL METHODS

Bilayers of  $\text{La}_{0.7}\text{Ca}_{0.3}\text{Mn}_3\text{O}/\text{Pr}_{1.85}\text{Ce}_{0.15}\text{CuO}_4$  (LCMO/PCCO) were prepared by pulsed laser deposition using a KrF excimer pulsed laser onto  $\text{NdGaO}_3$  (001) substrates without breaking vacuum. The 200-nm-thick PCCO was deposited first at 10 Hz with an incident beam energy density of  $1.5 \text{ Jcm}^{-2}$  in nitrous oxide ( $\text{N}_2\text{O}$ ) at 150 mTorr. The substrate temperature was 1080 K. The LCMO was deposited under identical conditions directly onto the PCCO. Once grown, the bilayers were cooled to room temperature in 200 mTorr of  $\text{N}_2\text{O}$ . A series of samples were grown with different LCMO thicknesses of 10, 15, 17, 20, 25, and 50 nm.

The LCMO/PCCO bilayers are epitaxial with a dominant (001)-orientation, as confirmed by x-ray diffraction. In Fig. 1, we have plotted the resistance-temperature dependence of an LCMO(15 nm)/PCCO(200 nm) film showing a change in slope at  $\sim 240$  K, which approximately coincides with the Curie temperature of LCMO. The PCCO had a critical superconducting temperature  $T_C$  of 17 K. The inset shows the magnetization vs in-plane field loop of the same film at 50 K, revealing a coercive field of 17 mT.

For STM, samples were transferred in dry atmosphere to a cryogenic system after a short ( $< 10$  min) exposure to ambient air. After evacuation, the STM chamber was filled with He exchange gas at 1 Torr and cooled to 4.2 K, where all the measurements presented here were performed using a Pt-Ir tip. Several measurements were performed at temperatures up

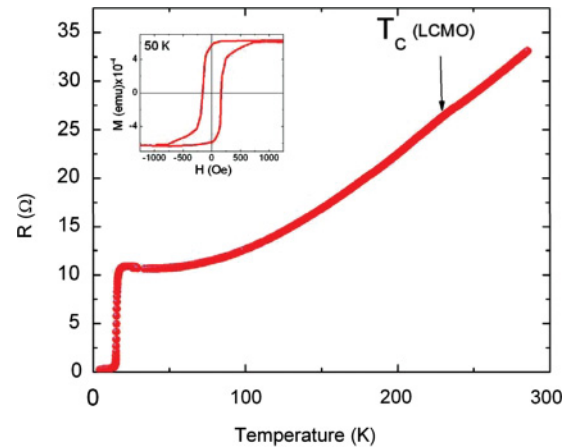


FIG. 1. (Color online) The resistance vs temperature of an LCMO(15 nm)/PCCO(200 nm) bilayer showing a change in slope at  $\sim 240$  K, which approximately coincides with the Curie temperature of LCMO and the critical superconducting temperature of PCCO of 17 K. The inset shows the field dependence of the magnetization of the bilayer at 50 K.

to 150 K to verify that the spectroscopic features associated with superconductivity (gaps and ZBCPs) indeed vanished above the  $T_C$  of PCCO. Topographic images were taken in the standard constant current mode with bias voltages of  $\sim 100$  mV, well above the superconducting gap voltage of PCCO. The tunneling conductance  $dI/dV$ - $V$  spectra (which reflect the local density of states, DoS), were numerically derived from the current-voltage ( $I$ - $V$ ) curves acquired on the LCMO surface while momentarily disconnecting the STM feedback loop.

## III. RESULTS

In Fig. 2, we have plotted the typical spectra acquired on bare PCCO at 4.2 K showing a superconducting gap of 3 mV. The data is fitted to the formulation introduced by Tanaka *et al.*<sup>35</sup> for tunneling into a  $d$ -wave superconductor where  $Z$  is the barrier strength parameter, including also a finite lifetime broadening Dynes parameter  $\Gamma$ .<sup>36</sup> We have also found areas showing shallower gaps (having larger zero-bias conductance) and also metallic regions, reflecting areas with suppressed surface superconductivity, probably due to surface contamination. This problem was avoided in the bilayer samples because the LCMO top layer protects the PCCO. It is important to note here that we did not find spectra exhibiting ZBCP on bare PCCO films, although many regions were scanned, including grain boundaries that may expose nodal facets. This is consistent with data reported previously for PCCO,<sup>34</sup> but it contrasts with STS measurements performed on  $c$ -axis YBCO films, where ZBCPs are commonly found on (110) and other (non antinodal) facets.<sup>37</sup> The STM image presented in the inset of Fig. 2 exhibits the crystallite structure of the bare PCCO film.

Figure 3 shows a topographic image of an LCMO (15 nm)/PCCO(200 nm) sample with spectra acquired on a  $100 \times 100 \text{ nm}^2$  area. Evidently, the surface morphology of the LCMO overlayer differs significantly from that of the bare

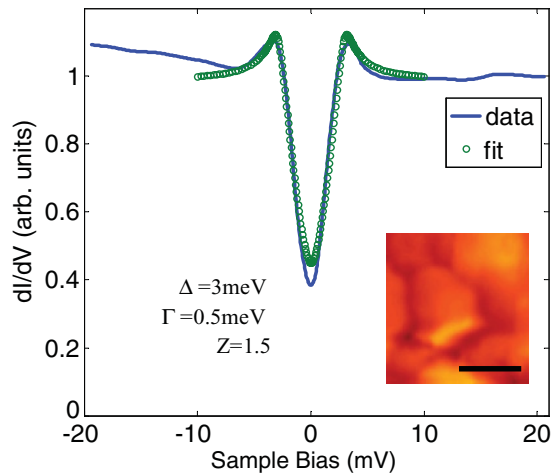


FIG. 2. (Color online) Tunneling spectrum acquired on a bare PCCO film at 4.2 K (solid blue curve). The fit (open circle green curve) was computed for *c*-axis tunneling into a *d*-wave superconductor including finite lifetime broadening effects. Here,  $\Delta$  is the gap,  $\Gamma$  is the Dynes broadening parameter, and  $Z$  is the barrier strength parameter (as described in the main text). No zero-bias conductance peaks were observed on the bare PCCO film, although many regions were scanned. The inset shows a typical topographic image of the bare PCCO film, 200 nm thick, manifesting its crystalline structure; scale bar is 300 nm.

PCCO film (see Fig. 2), being more granularlike. In this region, only gaps appeared in the tunneling spectra, such as the one shown in (a) and those shown in (b), which were consecutively acquired along the marked line depicted in the inset. Since the “gapped region” is quite large compared to the coherence length in PCCO ( $\sim 30$  nm) and the domain wall width ( $\sim 20$  nm), it seems that the PE here is not necessarily confined to domain walls. It is also important to note that no S-like features appeared at temperatures above the  $T_C$  of the PCCO or on the 50-nm LCMO/PCCO sample. The gap and

ZBCP features were checked for repeatability with respect to changing the bias and current set points in order to rule out single electron charging effects.<sup>38</sup>

Tunneling spectra featuring ZBCPs were found on LCMO/PCCO bilayers with 10-, 20- (not shown), and 25-nm-thick LCMO layers with typical shapes shown in Fig. 4. The ZBCPs were far less abundant compared to the gap features, as expected from the fragile nature of anisotropic superconductor order parameters. Curve (1) in Fig. 4(a) is an average over more than 10 normalized  $dI/dV$ - $V$  tunneling spectra (part of which are shown in the inset) acquired with different bias voltage and current set points on an LCMO(10 nm)/PCCO(200 nm) sample in the region indicated by the arrow in the inset of Fig. 4(b). The normalized spectra (to the dip at positive bias) and, in particular, the appearance of the ZBCP were insensitive to changes in the set points and thus reflect the intrinsic local DoS in that region and not single electron charging effects. The spectra in Fig. 4(b) were acquired on an LCMO(25 nm)/PCCO(200 nm) sample and show much smaller ZBCPs embedded inside sharp gaplike features, the origin of which will be discussed below. Since no ZBCPs were found on bare PCCO samples, these results strongly suggest that an intrinsic anisotropic order parameter is induced in the LCMO that is responsible for the appearance of the ZBCPs. It is important to note that, in some cases, ZBCPs were unstable against remeasurement using the same STM set points, turning into gapped or metalliclike spectra. Possible explanations for this behavior are given in the following section.

#### IV. DISCUSSION

Our results show evidence for long-ranged superconductivity in LCMO proximity coupled to a 200-nm-thick layer of superconducting PCCO. The conventional FFLO-like mechanism for singlet proximity effects in ferromagnets coupled to superconductors can explain penetration of a superconducting order into ferromagnets up to distances of

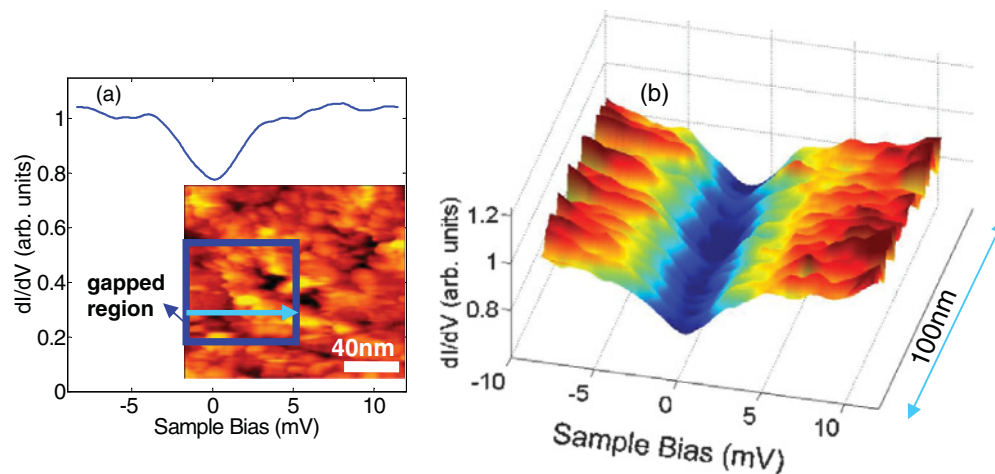


FIG. 3. (Color online) Scanning tunneling spectroscopy data measured at 4.2 K on LCMO(15 nm)/PCCO(200 nm) sample. (a) Representative tunneling spectrum acquired within the marked gapped region in the STM topography image shown in the inset. (b) Tunneling spectra acquired along the line indicated by the arrow on the topographic map in (a). All spectra data in the marked  $\sim 100 \times 100$  nm<sup>2</sup> region showed induced superconducting-like gaps similar to (a), indicative of a proximity effect. In the close environment of the gapped region, the spectra were metalliclike.

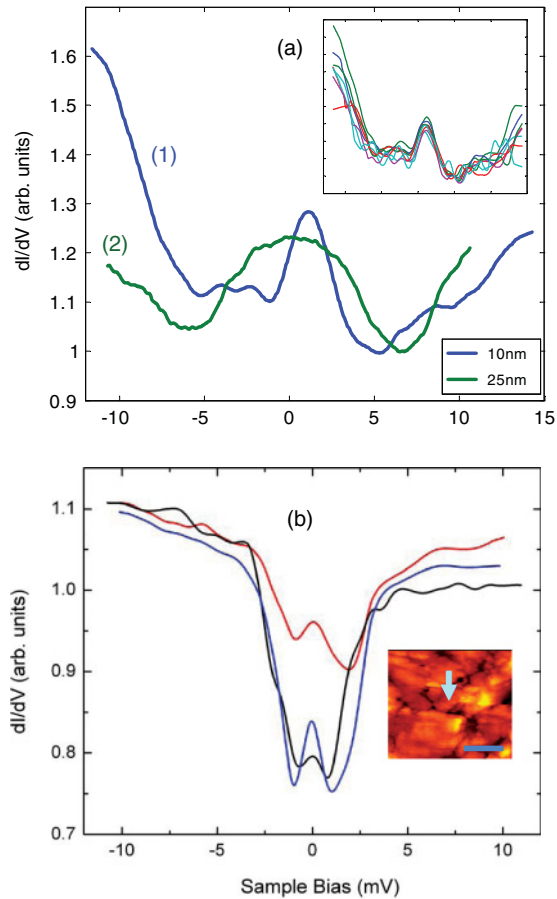


FIG. 4. (Color online) Tunneling spectra at 4.2 K showing ZBCPs. (a) Curve (1) is an average over normalized tunneling spectra acquired on a 10-nm LCMO/PCCO sample, while curve (2) was acquired on a 25-nm LCMO sample. (b) Tunneling spectra measured on a 25-nm LCMO/PCCO bilayer showing ZBCPs embedded in sharp gaplike features. The inset of (a) shows part of the spectra used to calculate curve (2). The spectra were measured over a region indicated by the arrow in the STM image presented in the inset of (b); scale bar is 50 nm.

only a few nanometers. Here, we observe proximity-induced gaps and ZBCPs in LCMO over tens of nanometers. Such a long-ranged proximity effect could in principle be explained in our system on the basis of CARE because the Cooper coherence length in PCCO is comparable to the domain wall width in LCMO; however, CARE cannot explain all the features observed in our results since it cannot account for the induced ZBCPs. In addition, the size of the gapped regions (see Fig. 3) were typically large compared to both the coherence length in PCCO and the domain wall width in LCMO, making CARE an unlikely mechanism to explain most of the results obtained here. Therefore, a more compelling explanation for the long-ranged proximity effect observed in LCMO is the formation of spin-aligned triplet-pairing correlations at the PCCO-LCMO interface, as indicated by our previous measurements on LCMO/YBCO bilayers, where CARE is not possible.

The question, therefore, that remains now regards the mechanism promoting the triplet-pairing, whether it is driven

by magnetic inhomogeneities in the LCMO, such as domain walls,<sup>39</sup> or spin-active interfaces<sup>2,3</sup> that can result from interdiffusion at the PCCO-LCMO interface leading, e.g. to uncompensated magnetic moments.<sup>2,40</sup> Since we did not find any gapped regions that could clearly be correlated with domain walls, it seems that the latter mechanism, involving spin-active interfaces, better accounts for our data. It should be noted, however, that this was not necessarily the case in the LCMO/YBCO bilayers where, in some cases, gaps were observed along strips of width comparable to that of the domain walls in LCMO, making the triplet-pairing mechanism suggested by Volkov and Efetov<sup>39</sup> highly likely. Further investigations are needed in order to fully resolve the main mechanism (or mechanisms) responsible for the long-range PE in the different systems studied by our group, LCMO/YBCO, LCMO/PCCO, and SrRuO<sub>3</sub>/YBCO bilayers.

We shall now discuss the possible orbital symmetries of the order parameters induced in the LCMO, as can be inferred by our results. In spin space, the triplet state is symmetric. As for the orbital symmetry of the induced OP, it was noted in Refs. 3, 28, and 41 that, in principle, anisotropic order parameters, such as  $p$  wave and  $d$  wave, can be induced along with an  $s$ -wave component. In order to maintain overall fermionic antisymmetry, even-parity orbital symmetries must be accompanied by an odd dependence of the wave function on the Matsubara frequency, as originally proposed by Berezinsky<sup>42</sup> for superfluid <sup>3</sup>He. Unlike the case of  $s$ -wave pairing, anisotropic OPs are sensitive to impurity scattering and are therefore expected to be less abundant than the  $s$ -wave component in dirty samples. As discussed earlier, a hallmark of a sign-changing anisotropic OP is the ZBCP found in tunneling spectra for specific tunneling directions (along the nodal direction for  $d$  wave and lobe direction for  $p$  wave); consequently, ZBCPs are expected to appear less abundantly than gaps, as was indeed the case in our samples. Examples for tunneling spectra exhibiting pronounced ZBCPs are given in Fig. 4(a), showing that an anisotropic order parameter can penetrate the LCMO, in some locations, up to thicknesses much larger than the singlet coherence length  $\xi_F$ . It was already noted that, as was the case in LCMO/YBCO bilayers,<sup>5</sup> tunneling spectra featuring ZBCPs were in some cases unstable against remeasurement, evolving into gapped or metalliclike spectra. This can be explained by the sensitivity of the anisotropic OP to disorder. A tunneling measurement can be perturbative enough to cause changes in local disorder, strongly affecting the anisotropic order parameter and thus modifying the local proximity effect and consequently the local DoS. Figure 4(b) shows small ZBCPs within sharp proximity gaps, which can be explained by a superposition of OPs of different symmetries having a relative intensity that might be determined by the local disorder. Such spectral features can also be observed in specific tunneling directions with respect to the order parameter axes (e.g. with respect to the nodal or antinodal directions, as noted above). Since different orbital symmetries can produce similar tunneling spectra depending on their orientation with respect to the tunneling direction, it would be difficult to distinguish between the different relevant orbital symmetries (or a superposition of them) by fitting the tunneling spectra.

In spite of the uncertainty in the exact OP symmetry associated with the ZBCPs, their appearance in this study on half metallic LCMO films thicker than the singlet coherence length is compelling evidence for an exotic proximity effect. Since we did not observe ZBCPs on bare PCCO (nor to our knowledge has anyone else), their presence in the tunneling spectra on LCMO/PCCO samples is indicative that the induced triplet superconducting order parameter in the LCMO layer is indeed genuinely anisotropic.

## V. SUMMARY

We have applied scanning tunneling spectroscopy on half metallic ferromagnet-superconductor bilayers (LCMO/PCCO) and observed superconducting-like features in the tunneling spectra at localized regions where the LCMO layer thickness greatly exceeded the expected singlet pairing

coherence length in LCMO. This long-ranged superconductor-ferromagnet proximity effect can be attributed to induced triplet-pairing correlations mediated by spin-active interfacial regions. Significantly, we have also observed ZBCPs in the tunneling spectra on the LCMO/PCCO samples, but not on the surface of bare PCCO. This provides compelling evidence to support an induced anisotropic triplet-pairing order parameter in the LCMO layer.

## ACKNOWLEDGMENTS

O.M. thanks support from the Deutsch-Israelische Projektkooperation program, the US-Israel Binational Science Foundation, and the Harry de Jur Chair in Applied Science. M.E., J.W.A.R., and M.G.B. thank the Leverhulme Trust and the Royal Society for financially supporting this work.

\*milode@vms.huji.ac.il

- <sup>1</sup>S. A. Wolf, D. D. Awschalom, R. A. Buhrman, J. M. Daughton, S. von Molnar, M. L. Roukes, A. Y. Chtchelkanova, and D. M. Treger, *Science* **294**, 1488 (2001).
- <sup>2</sup>M. Eschrig, J. Kopu, J. C. Cuevas, and G. Schon, *Phys. Rev. Lett.* **90**, 137003 (2003).
- <sup>3</sup>M. Eschrig and T. Lofwander, *Nat. Phys.* **4**, 138 (2008).
- <sup>4</sup>R. S. Keizer, S. T. B. Goennenwein, T. M. Klapwijk, G. X. Miao, G. Xiao, and A. Gupta, *Nature* **439**, 825 (2006).
- <sup>5</sup>Y. Kalcheim, T. Kirzhner, G. Koren, and O. Millo, *Phys. Rev. B* **83**, 064510 (2011).
- <sup>6</sup>L. N. Bulaevskii, A. I. Buzdin, and S. V. Panjukov, *Solid State Commun.* **44**, 539 (1982).
- <sup>7</sup>A. I. Buzdin, *Rev. Mod. Phys.* **77**, 935 (2005).
- <sup>8</sup>P. Fulde and R. A. Ferrell, *Phys. Rev.* **135**, A550 (1964).
- <sup>9</sup>A. I. Larkin and Y. N. Ovchinnikov, *Zh. Eksp. Teor. Phys.* **47**, (1964).
- <sup>10</sup>J. W. A. Robinson, S. Piano, G. Burnell, C. Bell, and M. G. Blamire, *Phys. Rev. Lett.* **97**, 177003 (2006).
- <sup>11</sup>A. A. Bannykh, J. Pfeiffer, V. S. Stolyarov, I. E. Batov, V. V. Ryazanov, and M. Weides, *Phys. Rev. B* **79**, 054501 (2009).
- <sup>12</sup>J. W. A. Robinson, G. B. Halász, A. I. Buzdin, and M. G. Blamire, *Phys. Rev. Lett.* **104**, 207001 (2010).
- <sup>13</sup>J. W. A. Robinson, Z. H. Barber, and M. G. Blamire, *Appl. Phys. Lett.* **95**, 192509 (2009).
- <sup>14</sup>V. A. Oboznov, V. V. Bol'ginov, A. K. Feofanov, V. V. Ryazanov, and A. I. Buzdin, *Phys. Rev. Lett.* **96**, 197003 (2006).
- <sup>15</sup>T. S. Khaire, W. P. Pratt Jr., and N. O. Birge, *Phys. Rev. B* **79**, 094523 (2009).
- <sup>16</sup>T. Kontos, M. Aprili, J. Lesueur, F. Genêt, B. Stephanidis, and R. Boursier, *Phys. Rev. Lett.* **89**, 137007 (2002).
- <sup>17</sup>Z. Sefrioui, D. Arias, V. Pena, J. E. Villegas, M. Varela, P. Prieto, C. Leon, J. L. Martinez, and J. Santamaria, *Phys. Rev. B* **67**, 214511 (2003).
- <sup>18</sup>Y. Blum, A. Tsukernik, M. Karpovskii, and A. Palevski, *Phys. Rev. Lett.* **89**, 187004 (2002).
- <sup>19</sup>T. Kontos, M. Aprili, J. Lesueur, and X. Grison, *Phys. Rev. Lett.* **86**, 304 (2001).

- <sup>20</sup>V. T. Petrashov, I. A. Sosnin, I. Cox, A. Parsons, and C. Troadec, *Phys. Rev. Lett.* **83**, 3281 (1999).
- <sup>21</sup>M. D. Lawrence and N. Giordano, *J. Phys. Condens. Matter* **11**, 1089 (1999).
- <sup>22</sup>M. S. Anwar, F. Czeschka, M. Hesselberth, M. Porcu, and J. Aarts, *Phys. Rev. B* **82**, 100501 (2010).
- <sup>23</sup>I. Sosnin, H. Cho, V. T. Petrashov, and A. F. Volkov, *Phys. Rev. Lett.* **96**, 157002 (2006).
- <sup>24</sup>M. Giroud, H. Courtois, K. Hasselbach, D. Mailly, and B. Pannetier, *Phys. Rev. B* **58**, R11872 (1998).
- <sup>25</sup>T. S. Khaire, M. A. Khasawneh, W. P. Pratt Jr., and N. O. Birge, *Phys. Rev. Lett.* **104**, 137002 (2010).
- <sup>26</sup>J. W. A. Robinson, J. D. S. Witt, and M. G. Blamire, *Science* **329**, 59 (2010).
- <sup>27</sup>D. Sprungmann, K. Westerholt, H. Zabel, M. Weides, and H. Kohlstedt, *Phys. Rev. B* **82**, 060505 (2010).
- <sup>28</sup>F. S. Bergeret, A. F. Volkov, and K. B. Efetov, *Rev. Mod. Phys.* **77**, 1321 (2005).
- <sup>29</sup>R. Balian and N. R. Werthamer, *Phys. Rev.* **131**, 1553 (1963); M. Sigrist and K. Ueda, *Rev. Mod. Phys.* **63**, 239 (1991).
- <sup>30</sup>J. M. Byers and M. E. Flatté, *Phys. Rev. Lett.* **74**, 306 (1995).
- <sup>31</sup>G. Deutscher and D. Feinberg, *Appl. Phys. Lett.* **76**, 487 (2000).
- <sup>32</sup>I. Asulin, O. Yuli, G. Koren, and O. Millo, *Phys. Rev. B* **74**, 092501 (2006).
- <sup>33</sup>M. Ziese, S. P. Sena, and H. J. Blythe, *J. Magn. Magn. Mater.* **202**, 292 (1999).
- <sup>34</sup>Y. Dagan, R. Beck, and R. L. Greene, *Phys. Rev. Lett.* **99**, 147004 (2007).
- <sup>35</sup>Y. Tanaka and S. Kashiwaya, *Phys. Rev. Lett.* **74**, 3451 (1995).
- <sup>36</sup>R. C. Dynes, V. Narayanamurti, and J. P. Garno, *Phys. Rev. Lett.* **41**, 1509 (1978).
- <sup>37</sup>A. Sharoni, G. Koren, and O. Millo, *Europhys. Lett.* **54**, 675 (2001).
- <sup>38</sup>A. E. Hanna and M. Tinkham, *Phys. Rev. B* **44**, 5919 (1991).
- <sup>39</sup>A. F. Volkov and K. B. Efetov, *Phys. Rev. Lett.* **102**, 077002 (2009).
- <sup>40</sup>J. Linder and A. Sudbø, *Phys. Rev. B* **82**, 020512 (2010).
- <sup>41</sup>M. Eschrig, T. Lofwander, T. Champel, J. C. Cuevas, J. Kopu, and G. Schon, *J. Low Temp. Phys.* **147**, 457 (2007).
- <sup>42</sup>V. L. Berezinskii, *Pis'ma Zh. Eksp. Teor. Fiz.* **20**, 628 (1974).